R. & M. No. 3228

MINISTRY OF AVIATION

AERONAUTICAL RESEARCH COUNCIL
REPORTS AND MEMORANDA

Performance of the 36 x 35 in. Slotted Transonic Working Section of the R.A.E. Bedford 3-ft Wind Tunnel

By E. P. SUTTON, M. T. CAIGER and A. STANBROOK

LONDON: HER MAJESTY'S STATIONERY OFFICE

1961

PRICE 9s. 6d. NET

Performance of the 36 x 35 in. Slotted Transonic Working Section of the R.A.E. Bedford 3-ft Wind Tunnel

By E. P. Sutton, M. T. Caiger and A. Stanbrook

Summary. A 36 × 35 in. transonic working section with slotted walls on all four sides is described. It is interchangeable with the original supersonic working section of the 3-ft. tunnel, and is used for tests at Mach numbers up to 1·25.

The performance of the working section is summarised, with particular attention to effects of varying the angles of inclination of the upper and lower walls to the tunnel axis.

---

1. *Introduction.* The Royal Aircraft Establishment Bedford 3-ft wind tunnel has been described briefly in Ref. 1. It is a variable-pressure wind tunnel with a closed return circuit, driven by two centrifugal compressors in series, and was designed in the first place for operation at supersonic Mach numbers between 1·3 and 2·0.

An account was given in Ref. 2 of the development of slotted side liners for the original supersonic working section, which enabled the tunnel to be operated at high subsonic and transonic speeds, up to a Mach number of about 1·15, at the expense of a reduction in working section width to 27 in. Useful work has been done with this temporary arrangement, but a larger and more permanent transonic working section has also now been built.

The new working section was designed on conservative lines, using slotted walls, as before[2], in preference to perforated walls. The walls were mounted in such a way as to make possible the substitution of perforated walls later if required. All four were slotted, and the working section was surrounded by a single plenum chamber. Extraction of air to a low pressure region at the beginning of the diffuser ('diffuser suction') was again employed as the means of adjusting the pressure in the plenum chamber, because a more than adequate pressure ratio was available from the main compressors for this purpose. The tunnel speed was controlled by the main compressor speed throughout the range.

Provision was made for varying the wall divergence (defined in this report as the angle of inclination of the upper and lower walls to the centre line of the tunnel) through a small range,

---

* Previously issued as R.A.E. Report No. Aero. 2622—A.R.C. 21,908.

from about $+0\cdot4$ deg to $-1\cdot0$ deg. Use was made of this, during the tests reported here, for an investigation of the effects of wall inclination on the tunnel calibration, flow uniformity, and pressure ratio. The main object of the provision was to allow the best wall setting for uniformity of flow to be chosen at any particular Mach number.

In Ref. 2, difficulties experienced in obtaining a sufficiently uniform flow in the earlier transonic working section were attributed to the shallowness of the plenum chambers of the slotted liners. The plenum chamber of the new working section was made considerably deeper, but there was evidence of a recurrence of the same effect. This is discussed in the report.

The slotted working section is now in use for tests at subsonic and transonic Mach numbers up to $1\cdot25$; the original supersonic working section continues to be employed for Mach numbers above $1\cdot3$.

2. *Description of the Working Section.* The working section and the model-support section immediately downstream of it are contained in two fabricated steel pressure shells, lined with wood to form the internal walls of the tunnel. Fig. 1 shows the general arrangement and some of the main dimensions, and photographs from upstream and downstream are reproduced in Fig. 2. The principal dimensions are given in Table 1.

The working section is about 36 in. square, and has eight slots 130 in. long. The plenum chamber, between the slotted walls and the shell, is about 12 in. in depth. Each wall consists of two plywood slats, the edges of which are shaped to form a slot down the centre-line of each wall and a slot of half the width in each corner. The arrangement can be seen in Fig. 2; the half-slots are at the edges of the top and bottom walls. The slots are tapered at their upstream ends, increasing in width from zero to $2\cdot38$ in. in the first 81 in. of their length. Fig. 3 shows the slot shape, which was based on shapes given in Ref. 3. The fully developed open area ratio is 10 per cent. Each slat is stiffened by two light alloy I-beams, supported from the shell at their ends. The slopes of the top and bottom walls can be varied through a small range by means of electric jacks, which support the walls at their downstream ends, and rotate them about pivots at their upstream ends, upstream of the beginning of the slots. The side walls are fixed and parallel. A top and bottom wall setting of $0\cdot25$ deg divergence relative to the tunnel centre-line was expected to compensate approximately for the rate of growth of the boundary layers on the slotted walls. The slat faces are finished to a high standard of surface flatness, but some of the earlier tests were made before the final finishing had been done; details of the state of the slats are given in Section 4.

Upstream of the slotted liners, the working-section shell is lined with fixed blocks which are faired to the slats, forming the downstream end of the contraction. The gaps between these blocks and the beginning of the slats are sealed with inflatable rubber seals[4]. At the downstream end of the slats there is a shallow open step on each wall (Fig. 1), through which air is extracted from the plenum chamber, and further linings form a short constant-area section of height and width $40\cdot5$ in. The ends of the slats and the beginning of the fixed liners are shaped as can be seen in Figs. 1 and 2 to improve the extraction and mixing of air from the plenum chamber.

The lining of the model-support section forms the beginning of the diffuser, with a mean rate of expansion, over a length of $141\cdot5$ inches, equivalent to that of a $1\cdot37$ deg semi-angle cone. It is shaped just downstream of the constant-area section to offset the blockage of the model-support strut. This strut, to which a 7-ft long sting is attached for model tests, is a 2-in. thick curved steel plate of 36 in. chord, passing through sealed slots in the top and bottom walls of the

2

pressure shell. It is carried on an external frame, pivoted at the sides of the tunnel in line with the centre of the model. The sting was not fitted during the tests described here, except for the pressure ratio measurements with model mentioned in Section 6.

For convenience in the description of the experimental results, the cross-section at which the slots begin is referred to below as the throat. The upstream part of the slotted section, in which at supersonic speeds the main stream expands through the slots, is referred to as the nozzle region, and the part between about 2 and 3 tunnel heights from the beginning of the slots, in which the flow is relatively uniform at all speeds, is referred to as the test section. (The position of the cross-section of minimum area varies with the angle of inclination of the upper and lower walls because the walls are very slightly curved at the upstream end. When these walls are set at an angle of divergence of $0 \cdot 25$ deg from the tunnel centre-line, it is a few inches downstream of the beginning of the slots.)

3. *Calibration Probe and Wall Pressure Tappings.* For the calibration of the test section, a motor-driven traversing probe was mounted on the model-support strut in place of the sting. The probe consisted of a pointed conical static head, with vertex angle 3 deg, on a long tapering support. Details are given in Fig. 4, including an enlarged view of the tip reproduced from a shadowgraph of the actual cone. A similar but not identical static head had previously been used in the calibration of the slotted working section of Ref. 2. The rear end of the support slid in bearings which allowed a fore-and-aft travel of about 30 in. The tapered support was cranked; by rotation of the probe, and by mounting it on both sides of the strut in turn, it was possible to obtain the seven traverse positions shown at the right of Fig. 4.

The probe drive was coupled, *via* a step-by-step transmitter, to the chart drive of a recorder, the pen of which was driven by an automatic capsule manometer[5] connected to the probe. There was considerable lag in the system due to the resistance of the connecting lead between the static holes of the probe and the automatic manometer. The speed of traverse was such that this lag had little effect on the amplitude of pressure variations recorded in the calibration, but did affect their plotted positions. This error was not very important, because the probe was used only to investigate the uniformity of the flow in the present tests and, at any particular Mach number, was always traversed in the same direction.

A line of static pressure holes, at 2 and 4 in. intervals was provided along one of the slats at the position shown in Fig. 1, extending from 8 in. upstream of the throat, through the nozzle region and test section, to a point 18 in. from the end of the slotted walls. For measurement of the plenum chamber pressure distribution there was a line of 7 pressure holes in the wall of the outer shell, near a corner, at approximately 18 in. intervals from the throat position. An additional hole in the plenum chamber, also near a corner of the pressure shell and 92 in. downstream of the throat position, was used for measurement of a static pressure datum. There was a further row of wall holes along one side of the fixed liners downstream of the slotted walls, extending into the beginning of the diffuser part of the model-support strut.

4. *Details of the Tests.* All measurements were made at selected constant values of a reference Mach number, M_R, defined as the Mach number corresponding to the datum static pressure, measured in the plenum chamber, and a total pressure measured in the settling chamber. This was approximately the same as the stream Mach number in the test section. The range of M_R was usually from $0 \cdot 9$ to $1 \cdot 25$, but for some of the tests the wider range from $0 \cdot 4$ to $1 \cdot 3$ was covered.

3

The settling chamber pressure was 33·3 in. of mercury for the greater part of the tests, giving a Reynolds number of 16×10^6, based on tunnel height, at a Mach number of 1·0. Additional measurements were made over a range of total pressures from 10 to 45 in. of mercury. The total temperature was approximately 25 deg C, and the absolute humidity was always less than 0·0002 lb of water per lb of air.

Streamwise Mach number distributions in the nozzle region and test section were determined from measurements of the wall pressure distribution, with the upper and lower walls divergent at angles of 0·4 deg, 0·25 deg, 0·0 deg, −0·25 deg, −0·5 deg and −1·0 deg to the centre-line. The pressure distributions along the plenum chamber and along the wall downstream of the slotted liners were also recorded.

When these wall pressure measurements were made, the final smoothing of the slotted walls had not been completed. Irregular surface waves were present, with wavelengths of the order of the tunnel height, half-amplitudes up to 0·012 in., local slopes up to 0·0025 radian, and local rates of change of slope of as much as 0·004 radian in 0·1 tunnel height. After further smoothing, the maximum amplitude of the waves was reduced to about 0·005 in. and the maximum local slope to about 0·0005 radian.

More detailed measurements of the uniformity of the Mach number distribution along and near the centre-line of the test section were obtained by use of the static probe, at wall divergence angles between 0·4 deg and −0·5 deg. The main traverses were made after the walls had been smoothed, but some comparative measurements were obtained to show the effect of waviness of the walls on the centre-line Mach number distribution. The probe was not calibrated, and no correction has been applied to the probe readings. The traverses were used to measure the uniformity of flow rather than the absolute level of Mach number. The Mach number indicated by the probe is believed to be close to the true local Mach number, however; the magnitude of the difference is discussed in Section 5.3.

Errors in Mach number attributable to inaccuracies in pressure measurement did not exceed $\pm 0·002$ in general, at a settling chamber pressure of 33·3 in. of mercury. The reference Mach number M_R could be set and maintained constant to within the accuracy of measurement.

The tunnel pressure ratio was determined as the ratio of the settling chamber pressure to the pressure at entry to the first compressor.

5. *Mach Number Distributions.*   5.1. *Streamwise Mach Number Distributions from Wall Pressures.*
Fig. 5 shows typical curves of Mach number distribution along the slotted working section, calculated from wall static pressure measurements obtained with the upper and lower walls divergent 0·25 deg from the centre-line.

The curves show no unusual features. At subsonic speeds the Mach number distribution was approximately uniform. When the reference Mach number was greater than 1, the main stream Mach number was just above 1 at the throat, and the flow accelerated along the nozzle region until the Mach number was approximately equal to M_R. From there downstream the Mach number remained roughly constant. Expansion to a Mach number of 1·1 required a length of about 18 in., or half the tunnel height from the throat; expansion to 1·2 required about 45 in., or 1·2 times the tunnel height; expansion to 1·3 required about 75 in., 2·1 times the tunnel height.

The waviness of the curves calls for explanation. Later measurements showed that it could largely be accounted for by the slight waviness of the walls described in Section 4, together with

4

imperfections of some of the static holes. These defects were fortunately not sufficient to obscure the main trends of variation of the shape of the distributions with Mach number and wall setting.

In Fig. 6 the Mach number distributions deduced from wall pressures at four wall settings are compared. Each group of curves was obtained at approximately the same value of the reference Mach number M_R. Consequently the Mach number distributions for the different wall settings tend to fall close together towards the downstream end, because the reference static pressure was measured near the downstream end of the plenum chamber.

Fig. 6 shows that the acceleration of the main stream to any given Mach number required a greater length of the slotted section when the upper and lower walls were convergent than when they were parallel or divergent, as is to be expected. Thus, when the reference Mach number was 1·1, for example, a Mach number of 1·1 was reached 15 in. from the throat with 0·4 deg wall divergence, 35 in. from the throat with the walls parallel, and 70 in. from the throat with either 0·5 deg or 1·0 deg convergence. Similarly, the point at which sonic speed was reached when M_R was greater than 1 was further downstream, the greater the angle of convergence. When the walls were parallel, the sonic point was almost exactly at the beginning of the slots, and with the walls divergent 0·4 deg it was a few inches further upstream. When the walls were convergent the sonic point was downstream of the throat, moving upstream with increasing reference Mach number. It will be seen that with the walls convergent the acceleration of the stream occupied the first 70 in. or so of the slotted section, whatever the reference Mach number.

With the walls set at 0·4 deg divergence, there was a tendency at the lower speeds for the Mach number to increase slightly beyond M_R near the beginning of the working section and then to decrease again. This did not happen when the walls were parallel or convergent. As far as can be seen, this over-expansion and recompression did not lead to any reduction in the uniformity of the flow further downstream in the test section; on the contrary, the waviness of the Mach number distribution in the test section at Mach number 1·1 was greater with the walls convergent.

A gradual recompression along the test section occurred at the higher Mach numbers. Converging the walls at a fixed reference Mach number had the same effect. This can be partly explained by reference to the shape of the pressure distribution in the plenum chamber, and will be discussed in the following section.

5.2. *Comparison of Main Stream and Plenum Chamber Pressure Distributions.* In Figs. 7a to d smoothed curves of the wall Mach number distributions, faired by eye through the experimental points from which Fig. 6 was obtained, have been plotted to a larger scale, and curves of the static pressure distribution along the outer wall of the plenum chamber have been superimposed for comparison. Both sets of curves will be discussed in the following as static pressure distributions; a scale of p/H is given on the right-hand side of the figures. The variation of plenum chamber pressure distribution with Mach number and wall angle is shown more clearly in Fig. 8, in which plenum chamber pressure distributions for three wall angles are compared. Note that Fig. 8 has been plotted with increasing pressure upwards, and also that the reason why the curves intersect consistently about 90 in. from the throat is that they were obtained at nominally equal values of M_R, and thus of plenum chamber pressure (measured 92 in. downstream of the throat).

Fig. 8 shows that the static pressure in the plenum chamber was approximately constant at the lower Mach numbers when the walls were set at angles between 0·4 deg divergence and 0·5 deg convergence. With increase either of wall convergence angle or of Mach number, a dip developed

5

in the pressure distribution; a positive pressure gradient appeared downstream of 40 to 60 in. from the throat, preceded by a very slight negative gradient upstream.

The manner in which the main stream pressure fell and approached the plenum chamber pressure in the nozzle region is clearly shown in Fig. 7, and has already been described. Downstream of this expansion the static pressure in the main stream remained higher than the plenum chamber pressure in general. When a positive pressure gradient existed in the downstream part of the plenum chamber, a similar pressure gradient was observed, downstream of the expansion, in the main stream. This was the gradual recompression referred to at the end of the previous section. Both the pressure gradient and the difference between main stream and plenum chamber pressures increased with wall convergence angle, and with Mach number.

The positive pressure difference between the main stream and the plenum chamber in the test section can be accounted for by the necessity for a continuing outflow through the slots to maintain the Mach number approximately constant, due to wall convergence, by the growth of the boundary layer, or by both of these together.

Regarding the pressure gradient, it may be noted that the plenum chamber pressure distributions are similar in shape to pressure distributions observed, over the whole Mach number range, in the very shallow plenum chambers of the slotted side liners described in Ref. 2. It was found there that a positive pressure gradient began, both in the plenum chamber and in the main stream, where the turbulent mixing region spreading from the slots had penetrated close to the outer walls of the plenum chambers. A similar pressure gradient is observed in the re-attachment region of the flow past a finite backward-facing step. It seems likely that the pressure gradient under consideration here was of the same kind, in spite of the provision of a greater plenum chamber depth, since it became steeper as the total flow through the slots was increased, either by an increase in Mach number or by convergence of the walls. (It must be mentioned, however, that no substantial variation in the steepness of the gradient was observed within the smaller Mach number range of the working section of Ref. 2, and that the effect of varying the wall inclination was barely examined there.) Some very limited observations which were made of the behaviour of tufts mounted in the plenum chamber were consistent with this explanation. The flow in the plenum chamber opposite the test section was in the main stream direction to within a few inches of the outer wall, and in the opposite direction close to the wall. The depth of the upstream flow appeared to decrease as the slotted walls were converged; but the tufts were too unsteady for any definite conclusions to be drawn (probably because the scale of turbulence in the mixing zone was very large).

It was possible to obtain a sufficiently uniform flow without difficulty when the walls were set at a small angle of divergence. If a uniform flow over the whole range of wall settings had been required, some such measure as the addition of perforated screens to suppress mixing at the slots[2] might have been taken, to eliminate the gradient.

5.3. *Mach Number Distribution from Probe Traverses in the Test Section.* Fig. 9 shows typical curves of Mach number distribution along the centre-line of the test section, obtained by traversing the calibrating probe. The traverses were made after the walls of the working section had been re-worked smooth and flat. A comparison of some of the results with curves obtained when the walls were still in their unfinished state, corresponding to the wall Mach number distribution curves previously presented, is made in Fig. 10.

The curves in Fig. 9 show that when the upper and lower walls were divergent $0 \cdot 25$ deg from the centre-line, the total variation in Mach number on the centre-line in a length of 16 in. did not exceed $0 \cdot 003$ at subsonic speeds and $0 \cdot 009$ at supersonic speeds up to a Mach number of $1 \cdot 2$. In a length of 30 in. the total variation was $0 \cdot 005$ at $M_R = 0 \cdot 9$, and still not more than $0 \cdot 009$ at $M_R = 1 \cdot 1$ and $1 \cdot 15$. At a reference Mach number of $1 \cdot 25$ there was a positive pressure gradient along the whole length of the centre-line traversed, resulting in a decrease in Mach number of $0 \cdot 026$ in 16 in. and $0 \cdot 036$ in 30 in.

It is interesting to see, in Fig. 10, how large an improvement was brought about by the final smoothing of the walls. At reference Mach numbers of $1 \cdot 10$ and $1 \cdot 15$ the variations in Mach number over a length of 30 in. were reduced from $0 \cdot 022$ to $0 \cdot 009$, and from $0 \cdot 019$ to $0 \cdot 007$, respectively.

The variation of the centre-line Mach number distribution with wall divergence angle is shown in Fig. 11 for four reference Mach numbers. At $M_R = 0 \cdot 9$, the wall divergence angle scarcely affected the uniformity of the flow. At $M_R = 1 \cdot 1$ and $1 \cdot 15$ the distributions with $0 \cdot 5$ deg convergence were less uniform than the distributions with $0 \cdot 25$ deg or $0 \cdot 4$ deg divergence. At $M_R = 1 \cdot 25$ a flatter distribution was obtained with $0 \cdot 4$ deg divergence than with settings between $0 \cdot 25$ deg divergence and $0 \cdot 5$ deg convergence, mainly because the gradient associated with the flow in the plenum chamber was less steep.

Finally, Fig. 12 compares six Mach number distributions on and off the centre-line in the test section with $0 \cdot 25$ deg divergence at a reference Mach number of $1 \cdot 1$. The variation over the whole region, 30 in. long by 10 in. wide by 5 in. high, was $0 \cdot 012$. This was the maximum variation observed at Mach numbers up to $1 \cdot 2$.

The wall settings chosen for model tests were $0 \cdot 25$ deg divergence at Mach numbers up to $1 \cdot 20$ and $0 \cdot 40$ deg divergence at a Mach number of $1 \cdot 25$. In a typical test, the variation in local Mach number over the region occupied by the model would not exceed $0 \cdot 010$ at Mach numbers up to $1 \cdot 2$, and about $0 \cdot 015$ at $1 \cdot 25$.

As stated in Section 4, no correction has been applied to the Mach number measured at the orifices of the conical probe to derive the true free stream Mach number. Fig. 13 shows the variation with reference Mach number of the difference between the probe Mach number reading at a point on the centre-line, 90 in. from the throat, and a mean Mach number from wall pressure measurements in the test section. (*See* Section 5.4.) This probably gives some indication of the order of magnitude of the correction to be applied at high subsonic Mach numbers, but at super-sonic Mach numbers the presence of concentrated disturbances in the flow caused the probe reading to vary in an irregular manner. The difference predicted by supersonic theory if the free stream Mach number is equal to the mean wall Mach number is shown as a chain-dotted line. The best calibration curve that can be inferred from these results is obtained by fairing the experimental curve at subsonic speeds to the theoretical curve at supersonic speeds.

5.4. *Mean Mach Number Calibration.* In the absence of a reliable probe calibration, it was assumed that the mean Mach number obtained from 9 wall pressure measurements at 2 in. intervals between 82 and 98 in. from the throat was a satisfactory measure of the mean Mach number at the model position.

The difference between the reference Mach number and this mean wall Mach number was measured over the Mach number range from $0 \cdot 4$ to $1 \cdot 2$ at four total pressures with the upper and

lower walls at a divergence angle of $0 \cdot 25$ deg. The results are plotted in Fig. 14. Within the order of experimental accuracy ($\pm$ about $0 \cdot 003$) they are sufficiently well represented for calibration purposes by

$$\Delta M = 0 \cdot 006 \, M_R$$

or

$$\text{Mean } M = 0 \cdot 994 \, M_R.$$

There appears to be a tendency for the correction required to M_R to decrease with decreasing total pressure, but the experimental accuracy was not high enough, particularly at the lowest total pressure, for this to be certain.

Fig. 15 shows how the difference between the reference Mach number and the mean wall Mach number varied with wall divergence angle. The values of $\Delta M/M_R$ plotted in Fig. 15 are mean values obtained from measurements over the limited Mach number range from $0 \cdot 9$ to $1 \cdot 1$. These were less accurate measurements, and the discrepancy between Figs. 14 and 15 in the results for $\theta = 0 \cdot 25$ deg is not significant. The difference ΔM increased as the walls were converged, rising to about $0 \cdot 02 \, M_R$ with $1 \cdot 0$ deg convergence.

A separate investigation of the effect of the presence of a model in the working section on the reference Mach number is described in Ref. 6. No significant effect was found.

6. *Pressure Ratio.* The tunnel pressure ratio was measured over a range of Mach number at four wall divergence angles. The results are plotted against Mach number in Fig. 16 and against wall angle in Fig. 17.

The pressure ratio required at a given Mach number increased rapidly with increasing wall convergence in general, particularly at supersonic speeds. Thus for a Mach number of $1 \cdot 1$ pressure ratios of $1 \cdot 17$ and $1 \cdot 30$ were required with the walls divergent $0 \cdot 4$ deg and convergent $1 \cdot 0$ deg respectively. A pressure ratio of $1 \cdot 25$, which was sufficient for a Mach number of $1 \cdot 25$ with the walls divergent $0 \cdot 4$ deg, gave a Mach number of only $1 \cdot 20$ with the walls parallel, $1 \cdot 12$ with $0 \cdot 5$ deg convergence, and $1 \cdot 03$ with $1 \cdot 0$ deg convergence. The rate of increase of pressure ratio with Mach number was also higher with the walls convergent than with the walls parallel or divergent. At Mach numbers of $0 \cdot 8$ and $0 \cdot 9$ there was little variation of pressure ratio with wall angle in the range from zero to $0 \cdot 5$ deg divergence.

The general increase of pressure ratio with wall convergence was probably due mainly to the increase in the mass flow to be extracted from the plenum chamber into the diffuser and re-energised by mixing, but partly also to a reduction in the efficiency of extraction and mixing as the step height at the ends of the upper and lower walls increased. Measurements of the pressure distribution along one wall of the tunnel in the constant-area section and into the beginning of the diffuser, of which typical results are reproduced in Fig. 18, showed that there was a large variation in the pressure recovery in the immediate neighbourhood of the end of the slotted walls as the wall setting was altered.

There was little variation of pressure ratio with total pressure. At a Mach number of $1 \cdot 2$ the increase in pressure ratio for a reduction of total pressure from $33 \cdot 3$ to 10 in. of mercury was rather less than $0 \cdot 01$.

The effect of the presence of a fairly large model is shown in Fig. 19. With the model at zero incidence the change in pressure ratio was too small to be measured, but with the model at about 10 deg incidence pressure ratios $0 \cdot 005$ to $0 \cdot 02$ greater than with the tunnel empty were required.

The frontal area of the model was approximately 0·5 per cent of the tunnel cross-section area. It had unswept wings of gross area 56 sq in.

The measured pressure ratios are high, even at subsonic Mach numbers with the walls slightly divergent, compared with pressure ratios measured in some other tunnels with slotted working sections. The explanation of this is partly to be found in the magnitude of the losses in the part of the return duct between the end of the first diffuser section and the point at which the downstream pressure was measured. It is estimated that a contribution of 0·02 to 0·03 to the pressure ratio can be attributed to these losses. (When the tunnel is operated at the higher supersonic speeds for which it was designed the losses in the return duct are much less important.)

Both the general level of pressure ratio and the rate of increase with wall convergence angle would be expected to be lower for a shorter slotted working section.

7. *Conclusions.* 7.1. A good standard of flow uniformity in the test section was obtained when the upper and lower walls were set at a small angle of divergence. The variations in Mach number in the region occupied by a typical model did not exceed about 0·01 at Mach numbers up to 1·2.

7.2. Slight waviness of the slotted walls had a marked effect on the uniformity of flow in the test section.

7.3. At Mach numbers of 1·2 and 1·25, and also at lower speeds when the upper and lower walls were convergent, there was a small positive pressure gradient along the test section, probably induced by the flow in the plenum chamber. Its magnitude increased with convergence angle and Mach number.

7.4. Apart from the variation due to this general gradient, the uniformity of the Mach number distribution in the test section was not very dependent on the wall setting in the range between 0·4 deg divergence and 1·0 deg convergence relative to the centre-line.

7.5. The Mach number deduced from static pressure measurements at the wall of the test section was always slightly lower than the reference Mach number corresponding to a static pressure measured in the plenum chamber. The difference was 0·006 at Mach numbers near unity with the upper and lower walls divergent 0·25 deg from the centre-line, increasing to nearly 0·02 with 1·0 deg convergence.

7.6. The tunnel pressure ratio varied steeply with the wall setting, particularly at supersonic speeds. For a Mach number of 1·1, for example, a pressure ratio of 1·30 was required with the upper and lower walls convergent 1·0 deg, but 1·17 was sufficient with 0·4 deg divergence.

LIST OF SYMBOLS

p Static pressure

p_R Static pressure at a hole in the wall of the plenum chamber 92 in. downstream of the throat

H Total pressure (assumed to be equal to settling chamber pressure)

M Mach number

M_{Probe} Mach number measured by probe, uncorrected for probe error

M_R Reference Mach number, corresponding to the ratio p_R/H

M_{Wall} Mean Mach number at the wall in the model test region, determined from measurements of static pressure distribution along a slat between 82 and 98 in. downstream of the throat

θ Angle between upper or lower slotted wall and centre-line of tunnel, positive with the walls divergent

λ Pressure ratio for operation of tunnel, defined as ratio of settling chamber pressure H to pressure just upstream of the first compressor

---

REFERENCES

No.	Author	Title, etc.
1	D. E. Morris	Calibration of the flow in the working section of the 3-ft × 3-ft tunnel National Aeronautical Establishment. A.R.C. C.P. 261. September, 1954.
2	E. P. Sutton	The development of slotted working-section liners for transonic operation of the R.A.E. Bedford 3-foot wind tunnel. A.R.C. R. & M. 3085. March, 1955.
3	R. H. Wright, V. S. Ritchie and A. O. Pearson	Characteristics of the Langley 8-foot transonic tunnel with slotted test section. N.A.C.A. Report 1389. 1958.
4	D. I. T. P. Llewelyn-Davies and M. T. Caiger	Leakage tests on solid and inflatable rubber seals designed for use in wind tunnels. Unpublished M.o.A. Report.
5	G. F. Midwood and R. W. Hayward	An automatic self-balancing capsule manometer. A.R.C. C.P. 231. July, 1955.
6	L. C. Squire and A. Stanbrook	The influence of a model on plenum chamber indication of Mach number in a slotted wall wind tunnel. A.R.C. C.P. 395. February, 1958.

TABLE 1

Principal Dimensions

Distance from throat (inches)	Main stream		Width (inches)
	Height (inches)		
	$\theta = 0$	$\theta = 0\cdot25$ deg	
0	34·64	34·84	36·00
90	34·64	35·62	36·00
122	34·64	35·90	36·00
130	35·26	36·59	36·62
131	42·0		42·0
138	40·5		40·5
162	40·5		40·5
171	40·88		42·75
304	46·5		46·5

(θ = Divergence angle of upper and lower wall relative to centre-line.)

Contraction ratio	41:1
Internal cross-section of pressure shell	60 inches square
Depth of plenum chamber	approximately 12 inches
Length of slots	130 inches
Width of parallel part of slot	2·38 inches
Open area ratio (at parallel part of slots)	10 per cent
Range of wall divergence angles	0·4 deg to −1·0 deg

11
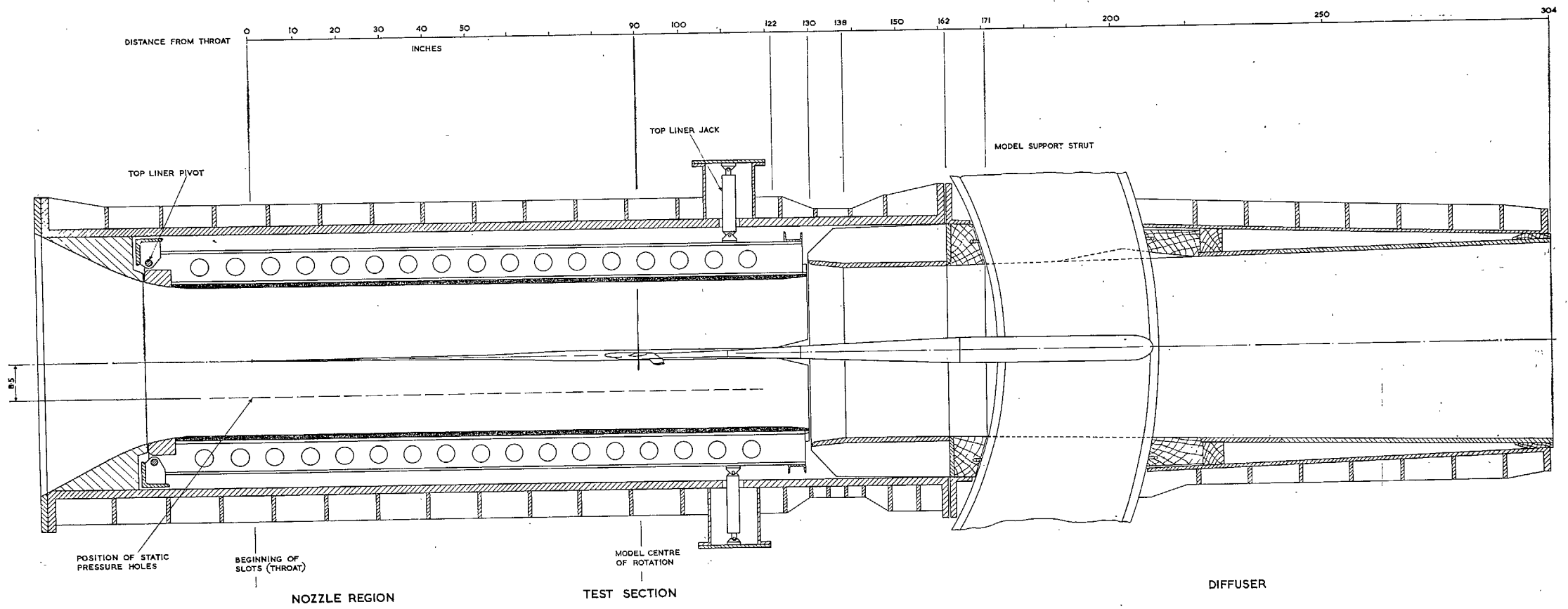
FIG. 1. Sectional elevation of working section, model support, and beginning of diffuser.

12
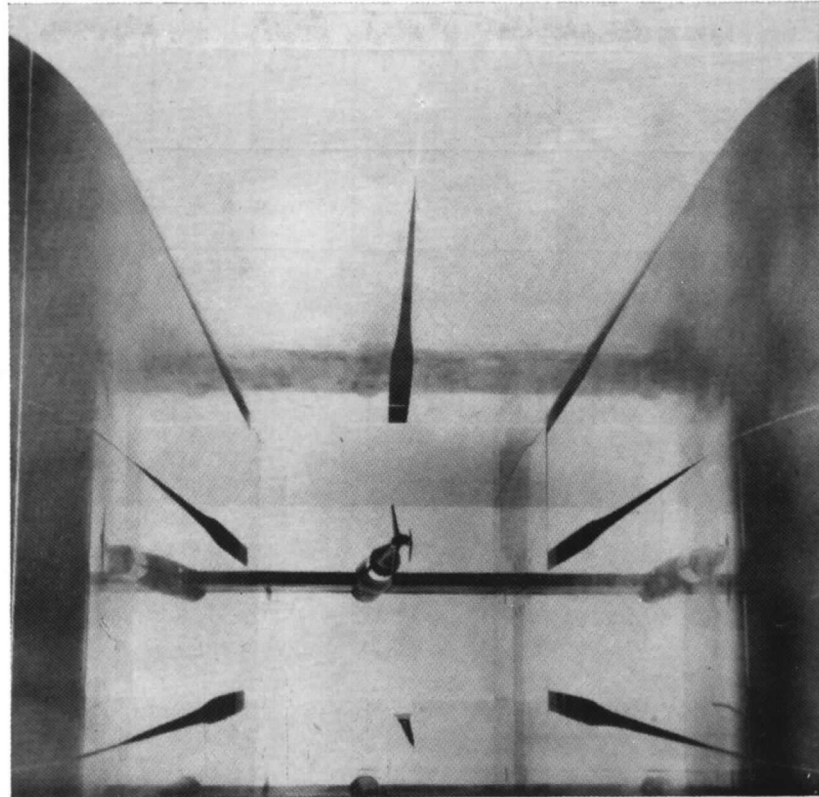
2a.   Working section and model-support section, from upstream.
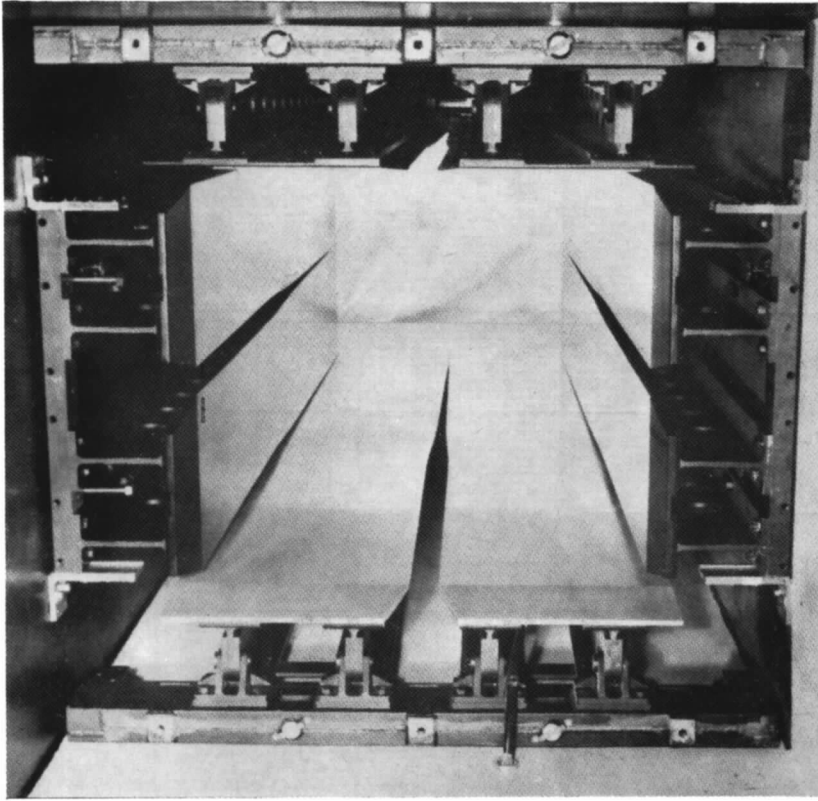
2b.   Slotted walls and pressure shell, from downstream.

FIGS. 2a and 2b.   Views of the working section.

13
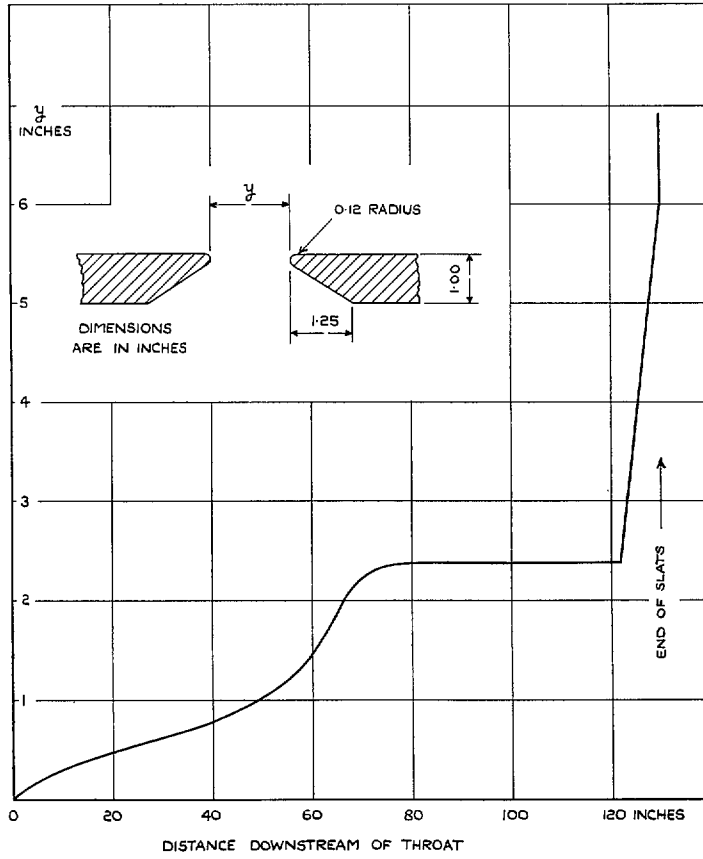
FIG. 3. Details of shape of slots.

14

Probe traverses 30 inches—
Sliding tube shown fully retracted

Enlarged detail of probe

3 holes
0·0135 inches dia.

3°

0·01 inch

0   0·5   1·0
inches

0   5   10
inches
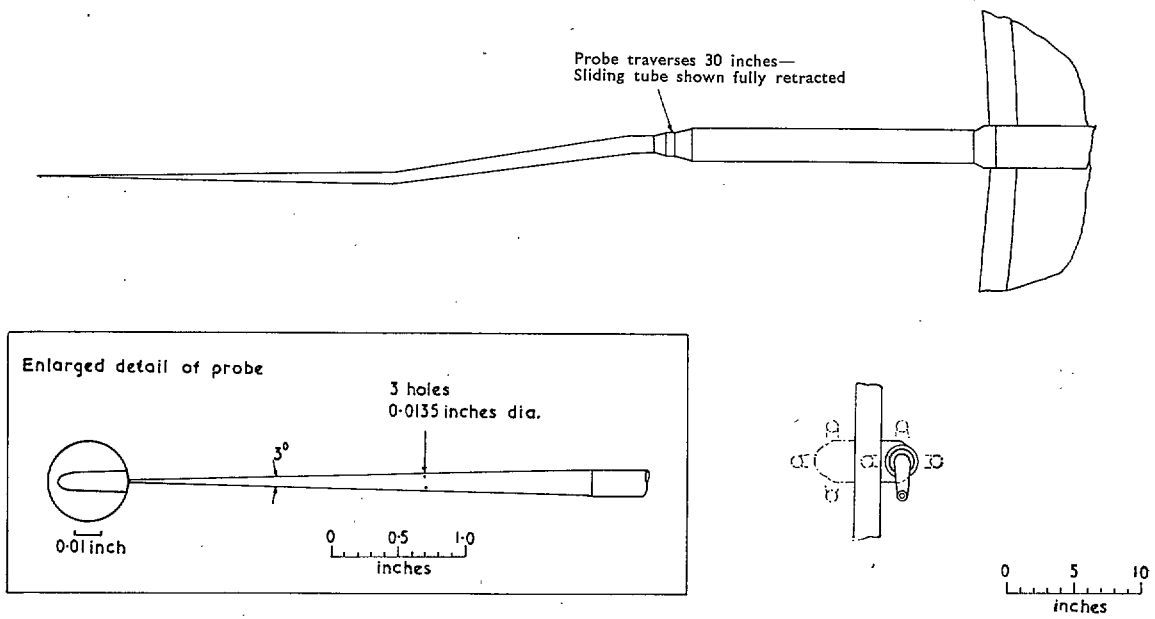
FIG. 4.   Calibrating probe.
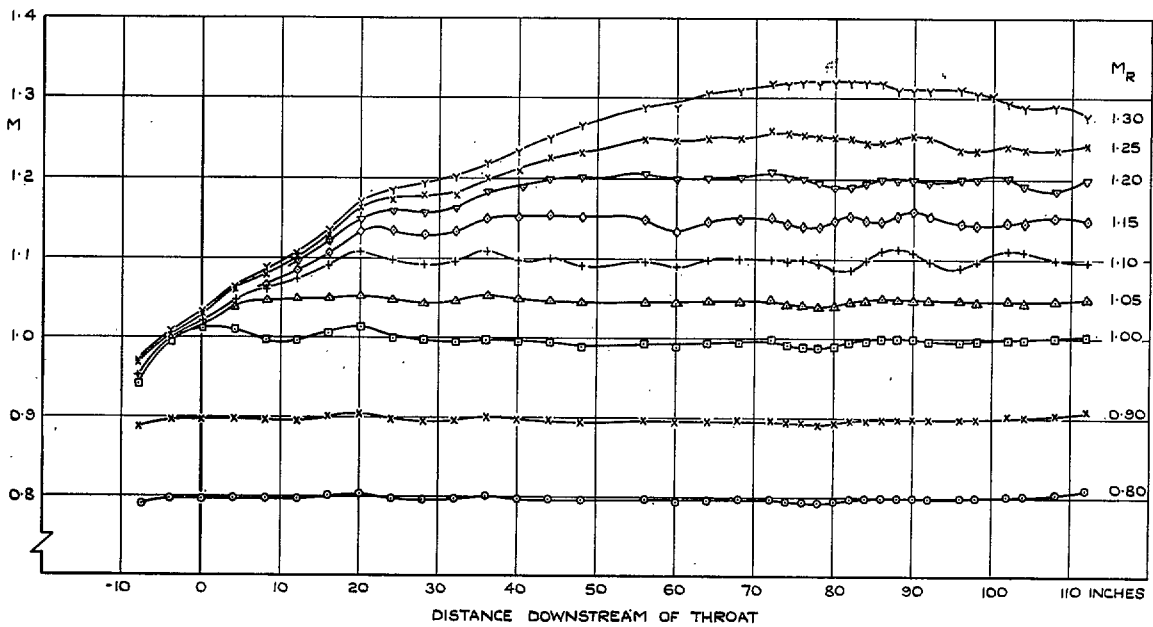
FIG. 5.   Wall Mach number distributions. $\theta = 0.25$ deg.

15
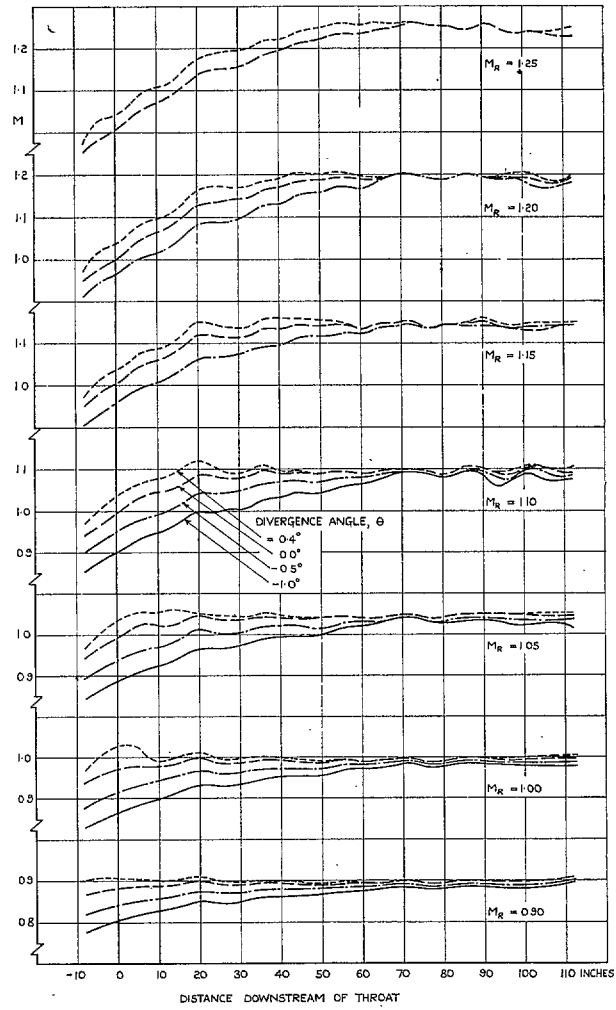
FIG. 6. Effect of wall inclination on wall Mach number distribution.

MAIN STREAM WALL
(FAIRED CURVES)

PLENUM CHAMBER

MAIN STREAM WALL
(FAIRED CURVES)

PLENUM CHAMBER

M

M

P/H

P/H

DISTANCE DOWNSTREAM OF THROAT

(a) $\theta = 0.4^0$

DISTANCE DOWNSTREAM OF THROAT.
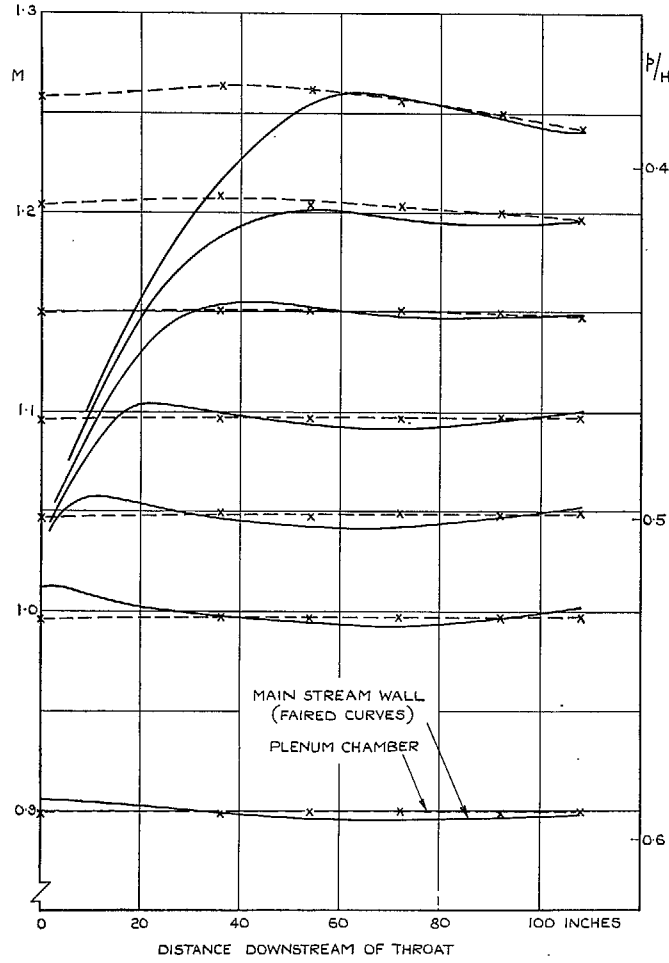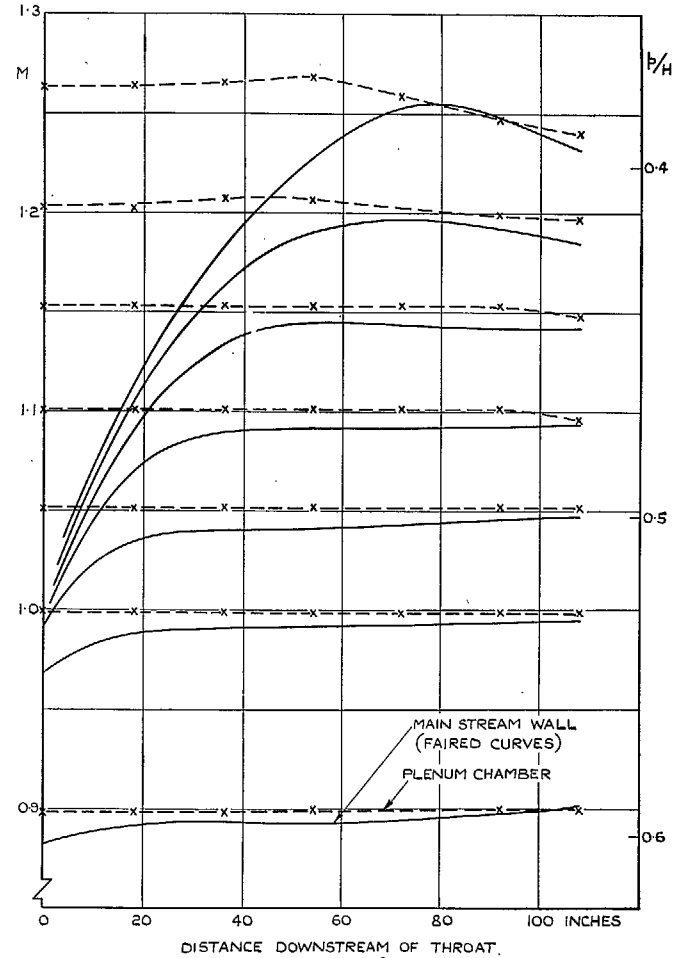
(b) $\theta = 0.0^0$

Figs. 7a and b. Comparison of main stream and plenum chamber pressure distributions.
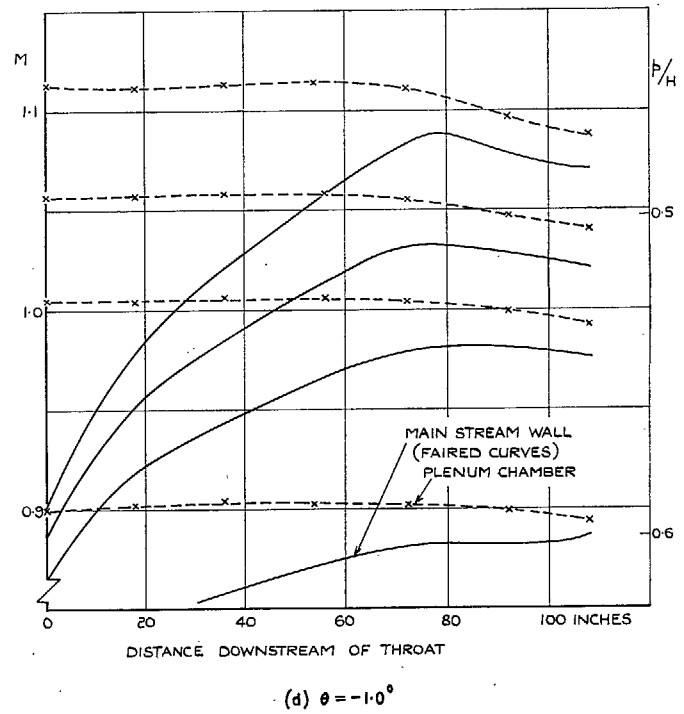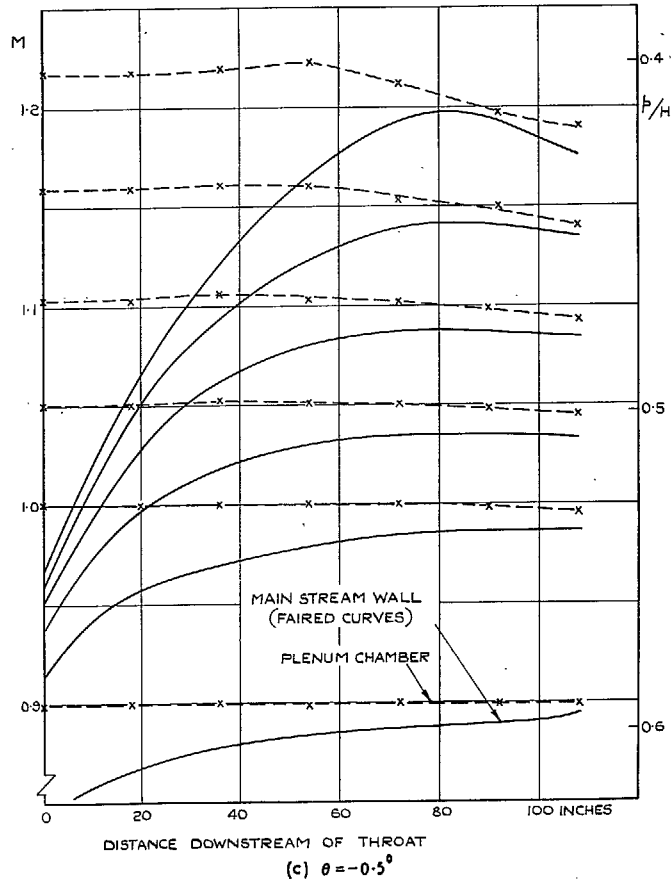
FIGS. 7c and d.   Comparison of main stream and plenum chamber pressure distributions.
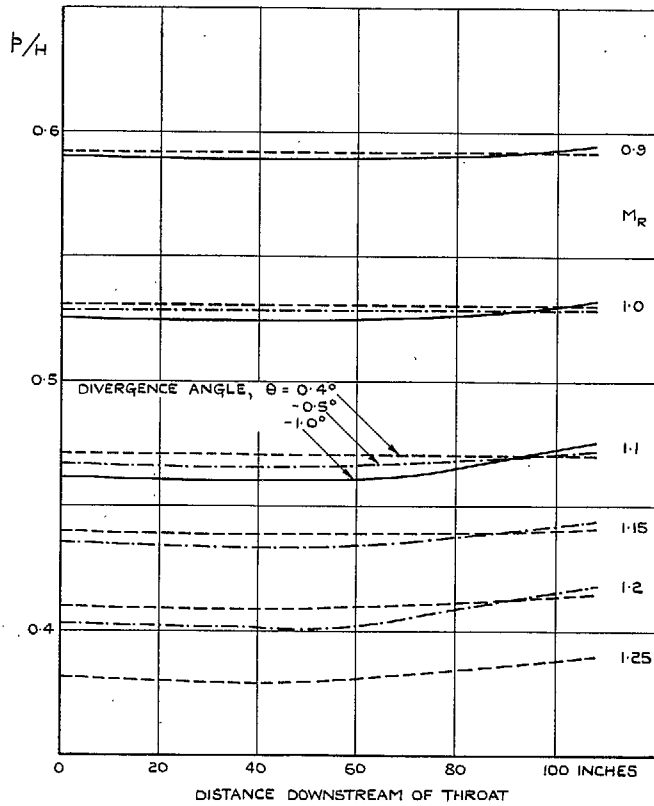
FIG. 8. Effect of wall inclination on pressure distribution along plenum chamber.
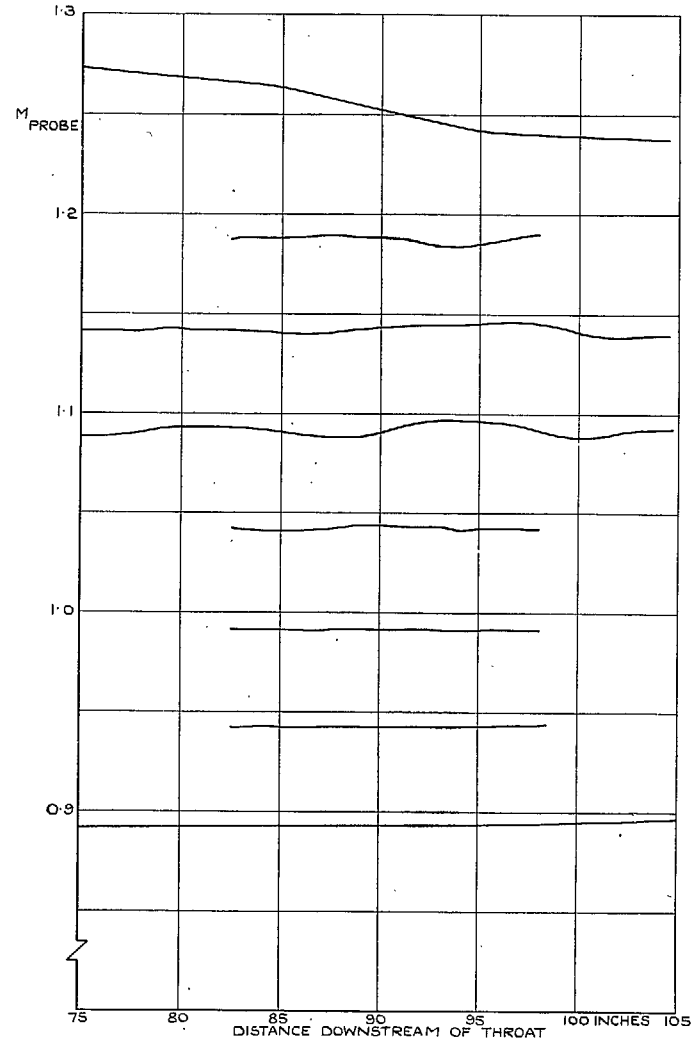
FIG. 9. Mach number distributions along tunnel centreline, from probe traverses. $\theta = 0.25$ deg.

19
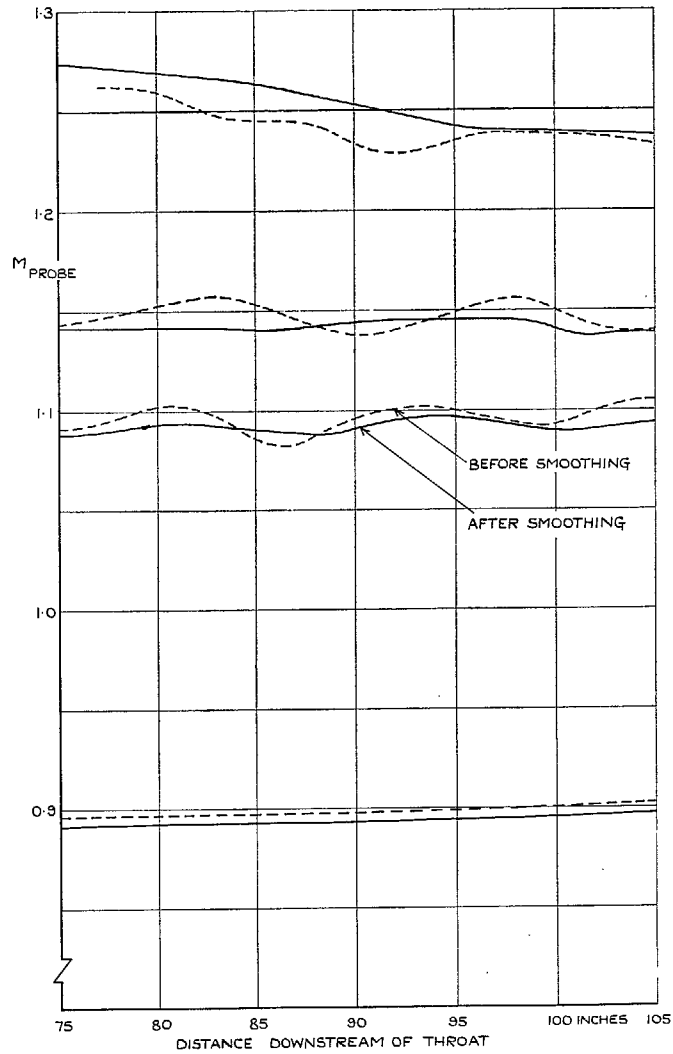
FIG. 10. Effect on centre-line Mach number distribu-
tion of smoothing working section walls. $\theta = 0 \cdot 25$ deg.
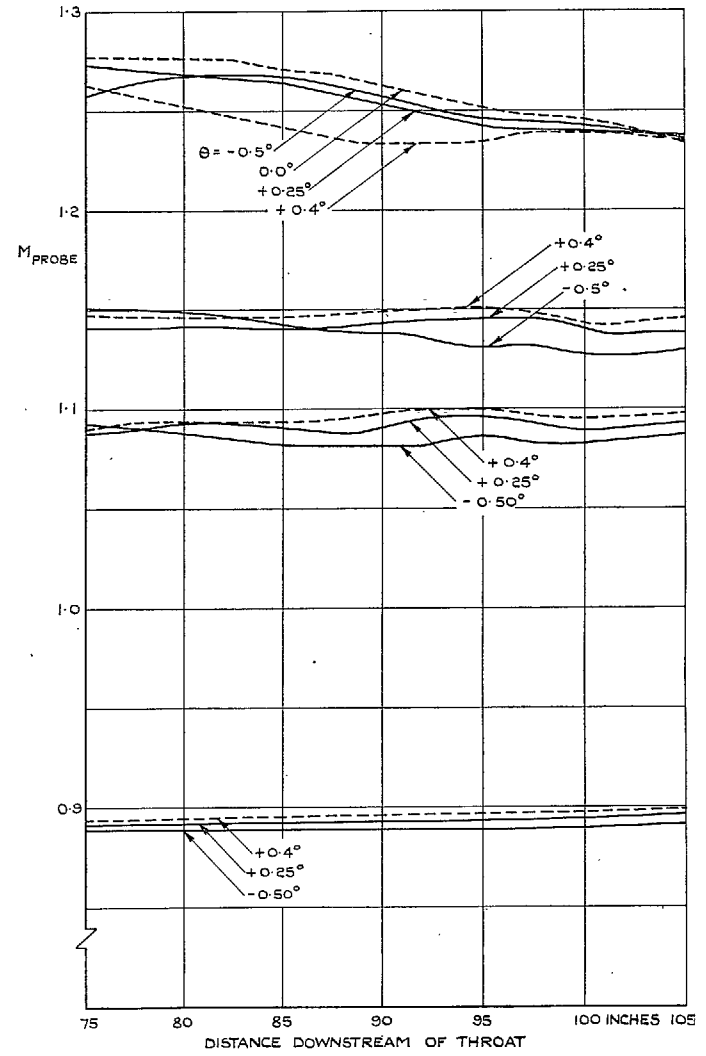
FIG. 11. Effect of wall inclination on Mach number
distributions along centre-line.
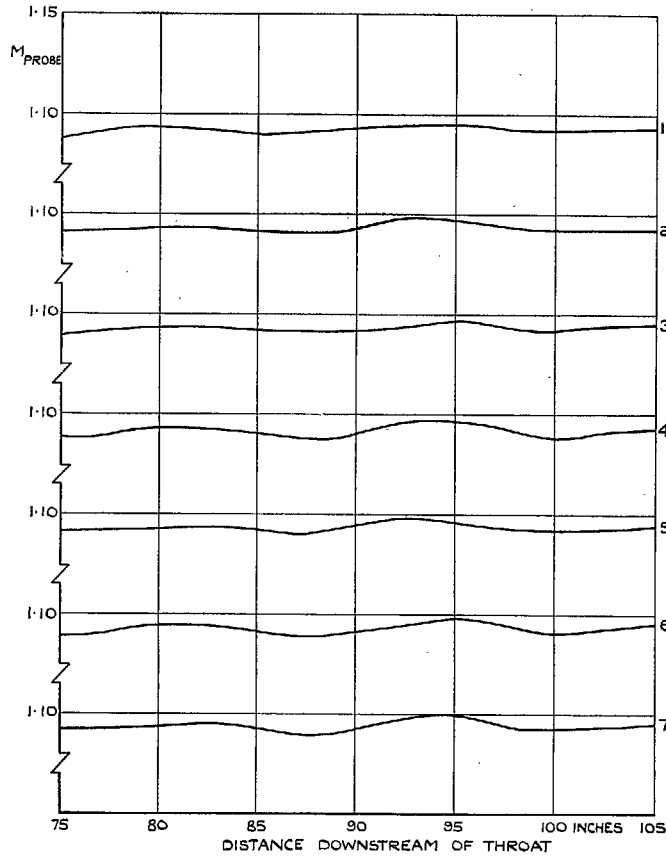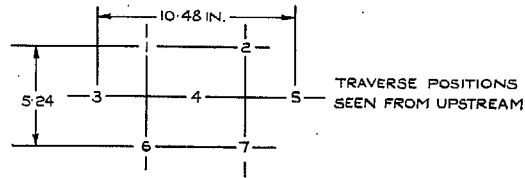
FIG. 12. Comparison of Mach number distributions on and off the centre-line. $M_R = 1 \cdot 1$, $\theta = 0 \cdot 25$ deg.
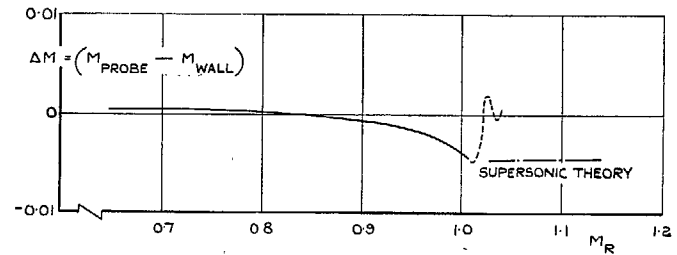
FIG. 13. Difference between probe Mach number at a fixed point and a mean wall Mach number. $\theta = 0 \cdot 25$ deg.
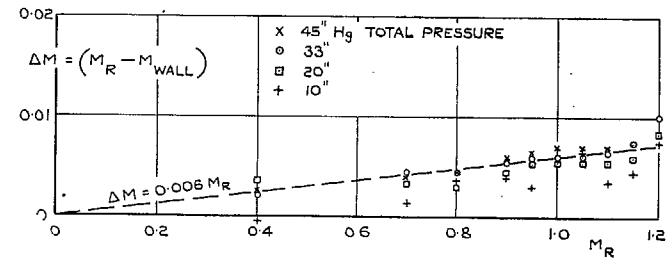

FIG. 14. Difference between M_R and a mean wall Mach number. $\theta = 0 \cdot 25$ deg.

$\left(\dfrac{\Delta M}{M} = \text{AVERAGE VALUE OF } \dfrac{M_R - M_{WALL}}{M_R} \text{ AT MACH NUMBERS} \right.$

$\left. \text{FROM } 0.9 \text{ TO } 1.1 ; \quad H = 33.3'' \text{ Hg} \right)$
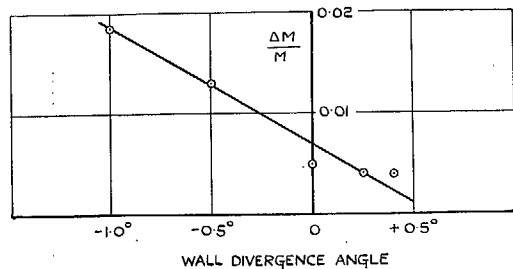

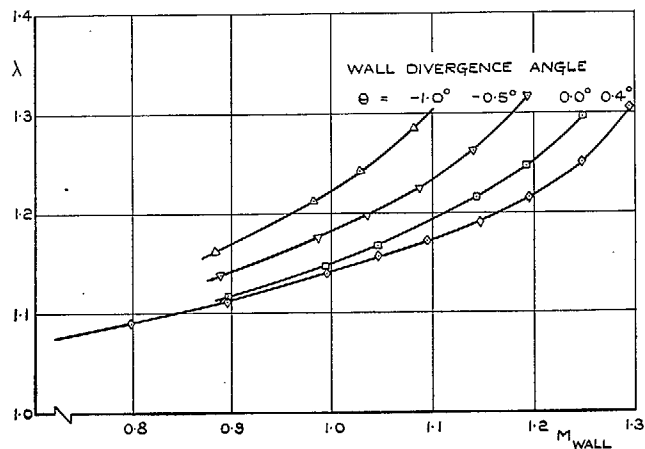FIG. 15. Variation with wall divergence angle of difference between M_R and a mean wall Mach number.

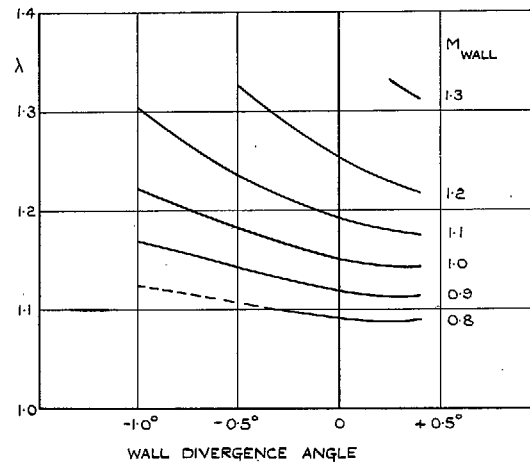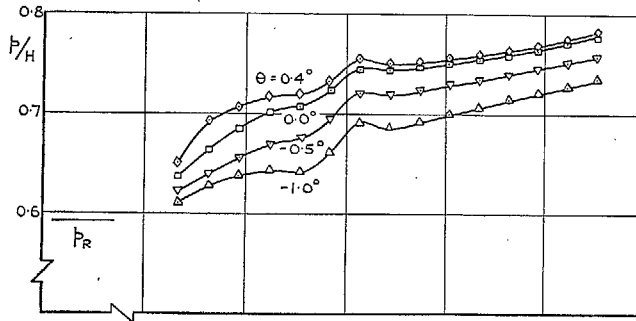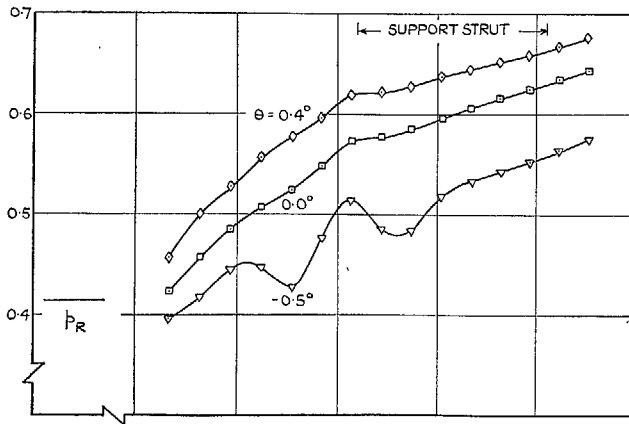FIG. 16. Pressure ratio λ at various wall settings.

FIG. 17. Effect of wall inclination on pressure ratio.

p/H

$0 \cdot 8$

$0 \cdot 7$

$\theta = 0 \cdot 4°$

$0 \cdot 0°$

$-0 \cdot 5°$

$-1 \cdot 0°$

$0 \cdot 6$

p_R

(a) $M_R = 0 \cdot 9$

$0 \cdot 7$

|← SUPPORT STRUT →|

$0 \cdot 6$

$\theta = 0 \cdot 4°$

$0 \cdot 0°$

$0 \cdot 5$

$-0 \cdot 5°$

$0 \cdot 4$

p_R

(b) $M_R = 1 \cdot 2$

FIG. 18. Typical wall pressure distributions downstream of slotted walls.

$1 \cdot 3$

λ

MODEL AT 10°
INCIDENCE

$1 \cdot 2$

WITHOUT MODEL,
AND WITH MODEL
AT ZERO INCIDENCE

$1 \cdot 1$

$1 \cdot 0$

$0 \cdot 9$ $1 \cdot 0$ $1 \cdot 1$ $1 \cdot 2$ $1 \cdot 3$
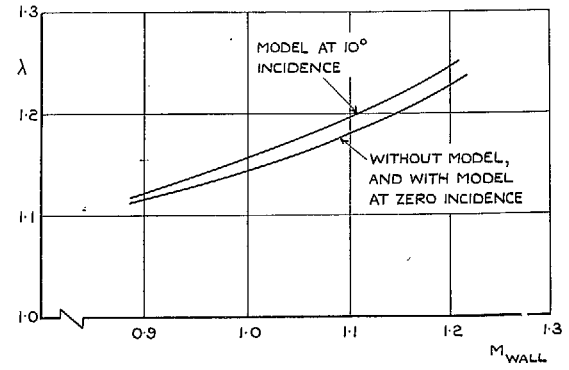
M_{WALL}

FIG. 19. Effect of a model on pressure ratio. $\theta = 0 \cdot 25$ deg. (Model wing area 56 sq in., blockage $0 \cdot 5$ per cent.)

Publications of the
Aeronautical Research Council

ANNUAL TECHNICAL REPORTS OF THE AERONAUTICAL
RESEARCH COUNCIL (BOUND VOLUMES)

1941 Aero and Hydrodynamics, Aerofoils, Airscrews, Engines, Flutter, Stability and Control, Structures.
63s. (post 2s. 3d.)

1942 Vol. I. Aero and Hydrodynamics, Aerofoils, Airscrews, Engines. 75s. (post 2s. 3d.)
Vol. II. Noise, Parachutes, Stability and Control, Structures, Vibration, Wind Tunnels. 47s. 6d. (post 1s. 9d.)

1943 Vol. I. Aerodynamics, Aerofoils, Airscrews. 80s. (post 2s.)
Vol. II. Engines, Flutter, Materials, Parachutes, Performance, Stability and Control, Structures.
90s. (post 2s. 3d.)

1944 Vol. I. Aero and Hydrodynamics, Aerofoils, Aircraft, Airscrews, Controls. 84s. (post 2s. 6d.)
Vol. II. Flutter and Vibration, Materials, Miscellaneous, Navigation, Parachutes, Performance, Plates and Panels, Stability, Structures, Test Equipment, Wind Tunnels. 84s. (post 2s. 6d.)

1945 Vol. I. Aero and Hydrodynamics, Aerofoils. 130s. (post 3s.)
Vol. II. Aircraft, Airscrews, Controls. 130s. (post 3s.)
Vol. III. Flutter and Vibration, Instruments, Miscellaneous, Parachutes, Plates and Panels, Propulsion.
130s. (post 2s. 9d.)
Vol. IV. Stability, Structures, Wind Tunnels, Wind Tunnel Technique. 130s. (post 2s. 9d.)

1946 Vol. I. Accidents, Aerodynamics, Aerofoils and Hydrofoils. 168s. (post 3s. 3d.)
Vol. II. Airscrews, Cabin Cooling, Chemical Hazards, Controls, Flames, Flutter, Helicopters, Instruments and Instrumentation, Interference, Jets, Miscellaneous, Parachutes. 168s. (post 2s. 9d.)
Vol. III. Performance, Propulsion, Seaplanes, Stability, Structures, Wind Tunnels. 168s. (post 3s.)

1947 Vol. I. Aerodynamics, Aerofoils, Aircraft. 168s. (post 3s. 3d.)
Vol. II. Airscrews and Rotors, Controls, Flutter, Materials, Miscellaneous, Parachutes, Propulsion, Seaplanes, Stability, Structures, Take-off and Landing. 168s. (post 3s. 3d.)

Special Volumes

Vol. I. Aero and Hydrodynamics, Aerofoils, Controls, Flutter, Kites, Parachutes, Performance, Propulsion, Stability. 126s. (post 2s. 6d.)
Vol. II. Aero and Hydrodynamics, Aerofoils, Airscrews, Controls, Flutter, Materials, Miscellaneous, Parachutes, Propulsion, Stability, Structures. 147s. (post 2s. 6d.)
Vol. III. Aero and Hydrodynamics, Aerofoils, Airscrews, Controls, Flutter, Kites, Miscellaneous, Parachutes, Propulsion, Seaplanes, Stability, Structures, Test Equipment. 189s. (post 3s. 3d.)

Reviews of the Aeronautical Research Council
1939-48   3s. (post 5d.)   1949-54   5s. (post 5d.)

Index to all Reports and Memoranda published in the Annual Technical Reports
1909-1947   R. & M. 2600   6s. (post 2d.)

Indexes to the Reports and Memoranda of the Aeronautical Research Council

Between Nos. 2351-2449   R. & M. No. 2450   2s. (post 2d.)
Between Nos. 2451-2549   R. & M. No. 2550   2s. 6d. (post 2d.)
Between Nos. 2551-2649   R. & M. No. 2650   2s. 6d. (post 2d.)
Between Nos. 2651-2749   R. & M. No. 2750   2s. 6d. (post 2d.)
Between Nos. 2751-2849   R. & M. No. 2850   2s. 6d. (post 2d.)
Between Nos. 2851-2949   R. & M. No. 2950   3s. (post 2d.)
Between Nos. 2951-3049   R. & M. No. 3050   3s. 6d. (post 2d.)

HER MAJESTY'S STATIONERY OFFICE
from the addresses overleaf